



Classification methods for detecting and evaluating changes in desertification-related features in arid and semiarid environments

Gabriela-Mihaela Afrasinei¹  · Maria Teresa Melis¹  · Cristina Buttau¹ · Claudio Arras^{1,2} · Marco Pistis¹  · Amar Zerrim³ · Messaoud Guied³ · Mohamed Ouessar³ · Bouajila Essifi³ · Mongi Ben Zaied³ · Amor Jlali³ · Hanen Jarray³ · Giorgio Ghiglieri^{1,2}

Received: 14 July 2016 / Accepted: 29 May 2017 / Published online: 27 June 2017
© Springer International Publishing Switzerland 2017

Abstract Land cover, land use, soil salinization, and sand encroachment, which are desertification-indicating features, were integrated in a diachronic assessment, obtaining quantitative and qualitative information on the ecological state of the land, particularly degradation tendencies. In arid and semi-arid study areas of Algeria and Tunisia, sustainable development requires the understanding of these dynamics as it withstands the monitoring of desertification processes. Both visual interpretation and automated classification approaches have been set up for salt and sand features extraction using historical and present Landsat imagery. The automated one includes a decision tree classifier and an unsupervised classification applied to the principal components extracted from Knepper ratios composite. New spectral indices are employed in the decision tree classifier for the

extraction of features of interest. The validation of the classification methods showed that the decision tree had an overall accuracy over 85% in both areas. Integrating results with ancillary spatial data, we could identify driving forces and estimate the metrics of desertification processes. In the Biskra area (Algeria), it emerged that the expansion of irrigated farmland in the past three decades has been contributing to an ongoing secondary salinization of soils, with an increase of over 75%. In the Oum Zessar area (Tunisia), there has been substantial change in several landscape components in the last decades related to increased anthropic pressure and settlement, agricultural policies, and national development strategies. One of the most concerning aspects is the expansion of sand-encroached areas over the last three decades of around 27%.

✉ Gabriela-Mihaela Afrasinei
afrasinei_gabriela@yahoo.com

Maria Teresa Melis
titimelis@unica.it; telegis@unica.it

Cristina Buttau
cbutttau@gmail.com

Claudio Arras
arrasclaudio@gmail.com

Marco Pistis
marpistis@virgilio.it

Amar Zerrim
zerrim1@yahoo.fr

Messaoud Guied
dagarimes@gmail.com

Mohamed Ouessar
ouessar.mohamed@ira.rnrt.tn

Bouajila Essifi
essifib@gmail.com

Mongi Ben Zaied
benzaied_m@yahoo.fr

Amor Jlali
jlali_amor@hotmail.com

Hanen Jarray
jarray_hanen@yahoo.fr

Giorgio Ghiglieri
ghiglieri@unica.it; nrd@uniss.it

¹ Department of Chemical and Geological Sciences, Lab. TeleGis, University of Cagliari, Via Trentino 51, 09127 Cagliari, Italy

² Desertification Research Center-NRD, University of Sassari, Viale Italia 39, 07100 Sassari, Italy

³ Institutes des Région Arides- IRA, Route du Djorf Km 22.5, Médenine, Tunisia

Keywords Salinization · Sand encroachment · Change detection · Landsat imagery classification · Land cover/use mapping · Decision tree

Introduction

Desertification phenomena and land-degradation processes threaten the sustainability and reliability of economic growth and monitoring is an indispensable requirement for reviewing and improving resource management. Natural and anthropic factors have a strong impact on the ecological state and quality of soils, especially in drylands where agricultural and animal husbandry practices are intensive, being the main branches of the local economy. Two major land-degradation phenomena interest the two arid and semi-arid study sites of Algeria (Biskra area) and Tunisia (Oum Zessar area): soil salinization and sand encroachment, respectively.

Indicators generally simplify reality to make complex processes quantifiable, thus the achieved information can be communicated (Jan et al. 2012). Common indicators of desertification include loss of biodiversity or declining habitat, loss of water-retention capacity, reduced soil fertility, and increasing wind and water erosion (Asfaw et al. 2016; De Waele et al. 2004; Lamchin et al. 2016). Therefore, soil salinization, sand encroachment, and vegetation cover changes are optimal land-degradation indicators and their monitoring is fundamental for the understanding of desertification dynamics. This paper focuses on the assessment of customized and replicable methodology and methods for the multi-temporal mapping of land-degradation indicators as high potential tools for monitoring and driving factors identification. Furthermore, the vast spatial and temporal coverage required for monitoring, the limited or no access to ground verification, and the need to cope with spectral confusion issues of desert land features require a proper approach (Eyal et al. 2008; Sheng et al. 2010; Muller and van Niekerk 2016a).

Salinity build-up is a concerning, increasing problem that has rendered impracticable extensive agricultural land, whereas soil salinization is present to different extents in more than 50% of the irrigated drylands (Fu et al. 2014; Masoud 2014; Singh 2015). It is a worldwide environmental issue that adversely affects plant growth, crop production, soil and water quality. Soil salinity is, in a first instance, a natural feature, an environmental hazard, but soil salinization is mainly a human—induced process, a form of land degradation that potentially leads to desertification (Gorji et al. 2015; Scudiero et al. 2015). Soil salinity and especially secondary salinization represent the main threat for sustainable agriculture in the Biskra region of Algeria.

As another form of land degradation, mainly reflecting excessive human activities and climate change in arid, semi-arid, and part of sub-humid region (UNCCD 2004), sand desertification has become worrying in the last decades especially in prone arid and semi-arid areas. Aeolian desertification is also one of the most devastating environmental and socio-economic problems in drylands, destroying land resources, reducing ecosystem productivity, depressing ecosystem services, and exacerbating poverty (Duan et al. 2014; Wang et al. 2015; Ge et al. 2016). Sand encroachment is one of the most serious environmental problems in south Tunisia and previous research shows that several unwary human activities have contributed to the intensification of this process, namely overgrazing, change in land use, and disturbances triggered by inappropriate agricultural practices or changes in socio-economic policies. In the Oum Zessar study area of south-eastern Tunisia, sand encroachment represents the main threat for the agro-pastoral activities, being the main branch of the economy of the whole Dahar-Jeffara Plain Medenine area (Ouassar 2007; Hanafi and Jauffret 2008; Sghaier et al. 2010; Ouerchefani et al. 2013; Ouassar et al. 2004; Afrasinei 2016). Since soil salinization is the second most important land-degradation indicator in this area, it was also taken into account in the classification analysis of this study.

The reason for choosing these two study areas, Biskra (Algeria) and Jeffara-Medenine-Dahar (Tunisia) is given by the fact that they reflect the main types of economic activities of high importance in North Africa: agro-pastoral activities, date palm monoculture-dominated (Occidental Zab, Biskra), open-field and industrial cultivation-dominated (Oriental Zab), and agro-pastoral, olive groves, small farming, fruit trees cultivation (Jeffara-Dahar). However, even if these activities are slightly different, these areas are similar in many aspects: similar bio-physical conditions, climatic and geomorphological characteristics (transition zone from lowlands to mountains, from rough desert to semi-arid conditions, though, in the case of Jeffara-Dahar area, the Mediterranean influences must be considered); similar geological features (predominance of carbonate rocks, formations rich in gypsum and halite, and similar continental deposits), both being characterized by the presence of chotts and sebkhas, even if, in one case, the situation is related to endorheic features (e.g., Chott Melrhir, Biskra) and, the other one, to coastal features (e.g., Sebkhia Oum Zessar, Jeffara area). Another reason for choosing these areas regarded the fact that, despite similarities, they presented two different main types of land-degradation phenomena, being the most representative ones for arid and semi-arid environments worldwide: soil salinization (secondary) and sand encroachment.

Remote sensing and the employment of geospatial tools have been confirmed as valid instruments and methods for diachronic analyses of desertification-indicators in order to support decision-makers. Salt and sandy features can be delineated and characterized spectrally based on the high content of main minerals when mapping using multi- or hyperspectral satellite imagery. The employment of change detection analysis offers the possibility to quantitatively and qualitatively estimate change rates and, therefore, argue driving factors (Fichera 2012; Melis et al. 2013; Vacca et al. 2014; Vogiatzakis and Melis 2015; Zewdie 2015). Common and acknowledged digital image classification methods, such as supervised, unsupervised, or spectral mixture, have been widely applied for the delineation of salt features, but no agreed-upon and replicable technique has been acknowledged to be optimal. The state-of-art reports problems regarding misclassification and spectral mix-up of salty features with other land cover types, especially urban features, bare land, and areas that have a high content of carbonate minerals (Khan et al. 2005; Fares and Philip 2008; Elnaggar and Noller 2010; Afrasinei et al. 2015a).

Various remote-sensing techniques and several spectral indices are proposed in the existing literature for the extraction of salt features in different types of areas, including drylands (Bouaziz et al. 2011; Sidike et al. 2014; Yahiaoui et al. 2015), but when these indices were applied in our study areas, results were not satisfactory, presenting problems of misclassification and spectral confusion. Consequently, in this study, we propose a customized decision tree classifier (Elnaggar and Noller 2010; Matthew 2012; Srimani and Prasad 2012) that copes with these issues, managing to delineate correctly 12 land cover classes and differentiate between two types of salt-affected areas: highly and moderately saline. We propose new indices to be employed in the decision tree classifier, which aim to cope with the issues risen by the study areas, in terms of well-known spectral confusion of highly reflective land features in semi-desert/desert areas.

A limited number of studies have been conducted in arid and semi-arid areas of Tunisia that approach sand encroachment and soil/groundwater salinization (Trabelsi et al. 2012; Lorenz et al. 2013; Ouerchefani et al. 2013; Msadki et al. 2014; Afrasinei et al. 2015b; Triki et al. 2016; Dhaou and Belghith 2009; Essifi et al. 2009; Afrasinei et al. 2017a; Triki Fourati et al. 2015), but they are employed at either local test sites or on a regional scale. Furthermore, results on driving forces and trends need more insight. The problem of differentiating desert sand from other sand surfaces from a spectral and mineralogical point of view was not approached until now. In this study, this distinction helped strengthen the understanding of their genesis, nature of driving factors, and environmental implications. We

argue that the contributing factors of sand encroachment expansion within the Jeffara Plain of northern Medenine governorate are primarily of anthropogenic nature and not of natural, windborne nature. We also argue that the Grand Oriental Erg is not the main source area of the inner-plain sandy areas of the Jeffara. In this sense, other studies argue that the aeolian sand transport in southern Tunisia is influenced by the predominant active winds ($u > 3 \text{ m}^{-1}$), coming from the east, southeast, and north, thus inducing a movement towards Sahara and not the opposite (Khatelli and Gabriels 2000). However, but more research needs to be undertaken and the results need further validation. Therefore, the same classification methods assessed and tailored for this study were applied in this second area, the Oum Zessar area of Tunisia. The particular aspect is that the same approach of decision tree construction provided valid results, successfully delineating two types of sandy features (desert sand and the inner-plain one). Furthermore, salt-affected areas and five other land-cover classes are identified, thus aiming at a rather high differentiation among land features. New indices are proposed also in this case, since the sandy features extraction was the main objective.

Band ratios are simple but highly efficient band operations that have been used also by the geological remote sensing community in order to identify hydrothermally altered minerals, hydrated sulfates and carbonates, and other types of land features. Specific red–green–blue (RGB) composites have been defined through the combination of various ratios, among which Knepper ratios. Up-to-date literature show that Knepper ratios have been used only in geological remote sensing until now (Mia and Fujimitsu 2012; Langford 2015; Afrasinei et al. 2017b). In this study, we propose its employment for salt and sand features extraction. In fact, the two automated classification schemes that are developed in this work comprise both (a) supervised multi-stage decision tree classifier (DT), and (b) unsupervised Iterative Self-Organizing Data (IsoData) classification applied to Principal Components (PC) of Knepper ratios (IsoData of Knepper PC). The reason why the latter one was also employed was to evaluate its potential as an approach of fast, automated, user-independent classifier, as opposed to decision tree analysis that needs thorough computation for rules choice and threshold calculation.

The methodological approach proposed in this study was also conceived because it is meant to be replicable in areas where historical data is scarce and the access to acquire field data is limited, either because the areas are remote/large or because of socio-political restrictions. In fact, due to the political and social context in Algeria, field survey was difficult to undertake personally and the amount of in-field acquired data was insufficient for a

proper validation. Therefore, in the case of the Biskra site, different stages of the analysis employed a large and complex set of auxiliary (NRD WADIS-MAR 2011), either extracted from pre-existing literature or employing community-generated data (Google Earth). In the Tunisian area, on the other hand, we were able to acquire thorough, systematically collected ground truth (GT) data, which supported both the visual and automated classification phases.

The present work proposes a versatile methodology for the qualitative and quantitative estimation of spatio-temporal variations of desertification phenomena in roughly accessible drylands. It comprises auxiliary, ground truth data, and remote-sensing methods.

The scope of this study was not only to map the land cover and soil conditions for a certain point in time but also to construct a customized and replicable methodology in order to repeat this investigation in different moments in time in similar environmentally sensitive areas and minimize previously reported issues of misclassification.

Consequently, we propose customized classification methods involving remote-sensing techniques and land cover and land use (LCLU) mapping through both visual interpretation and automated image classification methods. We put forward this approach in order to cope with limited access to ground truth data and minimize misclassification issues reported in the literature regarding the correct delineation of land cover features in desert areas. Furthermore, we needed to satisfy the requirement of extracting a higher number of land-cover classes than the average low number of classes (commonly between four and seven classes) usually obtained through traditional classification schemes at local–regional scales (Ceccarelli 2013; Nutini et al. 2013; Avelar and Tokarczyk 2014; Li 2014; Marconcini et al. 2014; Zhang et al. 2014). Moreover, several researchers have emphasized the importance of a polyvalent or hybrid methodological approach for mapping and detecting changes spatially and temporally with an increased accuracy (Aleksandrowicz et al. 2014; Olofsson et al. 2014; Zhu and Woodcock 2014).

The current research was undertaken in the framework of the Water Harvesting and Agricultural Techniques in Dry Lands: an Integrated and Sustainable model in MAghreb Regions (WADIS-MAR) Demonstration Project (www.wadismar.eu), funded through the Sustainable Water Integrated Management (SWIM) Programme, by the European Commission (www.swim-sm.eu). This project aims to achieve an integrated, sustainable, and participative water harvesting and water and agriculture management in the in the Biskra region of Algeria and the Dahar-Jeffara area (Oum Zessar study area) of central-eastern Tunisia, in the context of climate change, water scarcity, and human pressure accelerating ongoing land degradation

phenomena. Therefore, the purpose of this paper is to evaluate this latter aspect of indicators of land degradation, namely their delineation and spatio-temporal evaluation through proper classification methods.

Study sites

Wadi Biskra study area, Algeria

This study site, of approximately 5000 km², is located in the wilaya of Biskra, located at 500 km southeast of the capital Algiers (Algeria). Representing a vast piedmont area, it is delimited by the Aures mountainous domain in the north and by the Sahara plain in the south (Fig. 1a).

The area is also known as the *Zibans* (meaning *oasis* in Berber language), being possible to distinguish two agricultural sub-zones, the *Occidental Zab* or the *Zibans palmeraie* (meaning palm groves), based on date palm plantations and the *Oriental Zab* centered on open-field and industrial cultures. These latter cultures do not require a shallow aquifer (unlike phoeniculture) and this favored their expansion in the past 30 years, but instead they require deep pumping of groundwater that has a higher salinity than the shallow aquifers of the Occidental Zab.

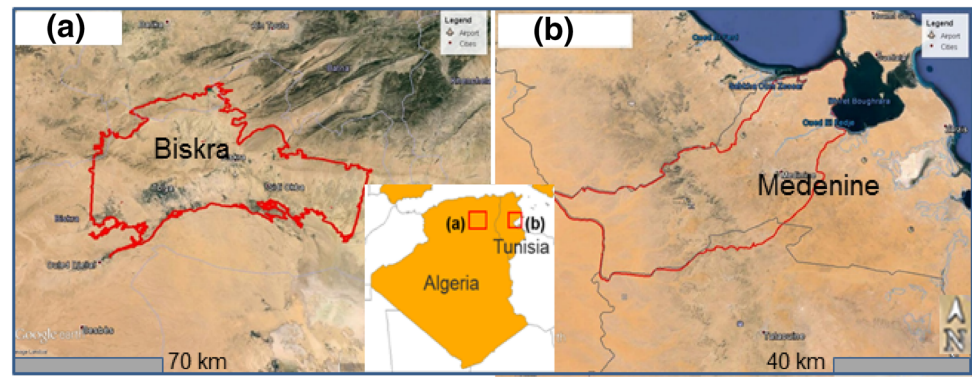
In the Occidental Zab, the highly productive and superficial aquifers (average salinity of 2–4 g/l) provide the conditions for a high production of high-quality dates, Deglet Nour. The irrigated area of around 70,000 ha has been reported to require the drawing of more than 600 million m³ per year (NRD WADIS-MAR 2011).

Various studies have focused on obtaining qualitative and quantitative parameters of these aquifers, some of which have employed up-to-date approaches of three-dimensional (3D) modeling, bringing to the attention of end-users their limited and fragile features (Buttau et al. 2013; Da Pelo et al. 2015; Arras et al. 2016).

From the geological point of view, the Biskra area is located at the southwestern boundary of the Aures Mountains (Saharan Atlas), between the folded Atlas domain in the northern part of the area and the Saharan desert and flat domain in the south. Its main lithological characteristics are given by the presence of Quaternary and Mio–Pliocene sands and clays, Mid-Eocene gypsum clays and evaporitic deposits, Lower Eocene limestone, gypsum clays and halite, Turonian dolomitic limestone and dolomites, and Cenomanian clay, marlstone and gypsum.

The economy of the Biskra region is agricultural-based and it represents one of the most important date palm producer and exporter at national but also international scale. In order to cope with increasing production demand and population needs, agricultural activities intensified, over-soliciting already fragile soils. Moreover, the climatic

Fig. 1 Study areas: Biskra, Algeria (a) and Oum Zessar, Tunisia (b). Base map modified from Google Earth



setting predisposes the concentration of salts in ephemeral surficial and slow-flowing underground waters that eventually are brought to surface through seepage due to excessive evapotranspiration, thus favoring salt crust formation (Fares and Philip 2008).

The climatic regime of this area is hot and dry, with an average annual temperature of about 22 °C, with a total annual rainfall average of approximately 150 mm. However, the average rainfall within a year is less than 20 mm. The minimum rainfall is almost zero in the months of July and August and the maximum occur in March and November.

Oum Zessar study area, Tunisia

The area of about 4000 km² mainly overlaps the northern part of the Médenine Governorate and stretches from the Great Oriental Erg in the west and crosses the Dahar Plateau and Jeffara Plain, reaching the Mediterranean Sea to the east (Fig. 1b). In this paper, for easiness of expression, it is denominated generically “Oum Zessar area” because it comprises the whole Oum Zessar watershed (of about 35,000 ha, in the north-western part of the study area), and it bares its name due to its importance for optimal characteristics for water supply in the surrounding area.

The main land-use types include extended rangelands, extended olive groves (mainly in the Jeffara Plain), local-scale arboriculture, episodic cereals, and small-farming irrigated agriculture. Crop sites, mainly arboriculture, are mainly found within torrential bodies behind water-harvesting structures: *jessour* and *tabias* (Graaff and Ouessar 2002; Schiettecatte et al. 2005), which are favored by the geomorphological context of the area, such as a high presence of alluvial landforms and paleo-valleys (Marini et al. 2008; De Waele et al. 2004).

The geological setting is given by the (1) Mesozoic deposits outcropping mainly in the Dahar domain, underlining for the current study the importance of the Cretaceous carbonate deposits with gypsum intercalations and (2) Mio-Pliocene continental deposits and Quaternary

alluvial and aeolian deposits found mainly in the Jeffara Plain. The shallow aquifers of the Mio-Plio-Quaternary deposits and the Turonian dolomitic limestone are exploited for the domestic use, with a salinity that ranges from 0.6 to 5 g/l. The water table ranges from 30 to 2–3 m near the coastal plain. The area receives between 150 and 240 mm of total annual rainfall and is defined by mild to cold winters and warm to very hot summers (up to 48 °C), with almost no rainfall from June to August.

Methodology and dataset

Methodological workflow

There are two commonly used remote-sensing mapping methods. One involves visual interpretation based on professional knowledge, and the other one is represented by automated classifications based on the use of computers. Visual interpretation focuses more on the applications and the automated method more on technological research (Zhang et al. 2014). In this study, the methodological approach was tailored considering several criteria based on the objectives of this work and the issues aimed to solve. It has been approached from both the theoretical and empirical perspectives. The theoretical one refers to the existing environmental problem of salinity and sand encroachment. It also refers to the analysis approach that the state-of-art literature recommends when attempting to define current state, driving forces, and the trends of these phenomena. These approaches are usually hybrid, and can include geospatial data, spectral/mineral laboratory and field measurements, ground data, remote-sensing data and techniques, geo-statistics, etc. The empirical perspective refers to the more technical part, thus image processing, classification method, and spectral analysis techniques. This latter one is necessary because it addresses the spectral confusion issue that is very common among desert features, as they are very reflective. Our methodological approach infers also the availability of ancillary data, the difficulty or

impossibility to acquire ground data, and misclassification issues.

In the present study, the visual interpretation particularly infers the lack of updated cartography at the local scale (or the regional scale), as well as the lack of spatial coverage of pre-existing cartography. Therefore, the mapping schema refers to the employment of two different classification approaches (visual and automated) or, in other words, three different classification methods: (a) on-screen visual interpretation mapping and (b) two automated classifications, namely a supervised one and an unsupervised one.

The first phase of this research consisted of the visual interpretation mapping land cover/land use features, and the creation of a nomenclature according to acknowledged guidelines in the literature. This phase was essential for the comprehensive knowledge of the areas and the generation of detailed LCLU maps (37 classes, scale 1:70,000), used as support and base map for the following analysis phases.

Secondly, two different automated classifiers were assessed, designed and applied, in accordance to reported limitations of various experimented classification methods in similar case study contexts by the scientific community (Pal and Mather 2003; Elnaggar and Noller 2010): (a) the decision tree classifier (DT) and (b) a customized unsupervised classification method (IsoData of Knepper PC). These were applied to the Landsat data acquired in 1984 and 2015 in the Biskra area, and in 1984 and 2014 in the Oum Zessar area in order to evaluate the change in land cover types over a maximum time span possible. In this sense, the aim was to employ the oldest and the most recent scenes available. In both areas, the 1984 Landsat scenes were the oldest available ones in terms of quality and lowest cloud coverage. In the Biskra area, the most recent one and the most adequate in terms of quality was the 2015 one (at the starting point of this research) and in the Oum Zessar area, the June 2014 scenes were chosen because their perfect overlap with the ground truth campaign that took place in June 2014.

Thirdly, the visual and automated classification maps were validated in both areas applying a confusion matrix (table of contingency calculated by comparing the results of the classification and the verification samples) using ground truth regions of interest (ROIs). In the Biskra area, the validation phase employed ground truth data composed of: (a) 46 field points acquired in 2013 (through the Algerian WADIS-MAR Project), (b) 83 points of soil profiles (each sampling site containing information on land-cover types, morphology, type of vegetation, soil texture, structure, soil type, soil group, etc.) and (c) 30 Google Earth points. In the Oum Zessar area, the 400 ground truth points were collected personally during the field campaign of June 2014. Half of these were employed

for the definition of training areas and the other half for the validation of the three classification methods.

In the last phase, change detection analysis was applied in both cases. The results are discussed through correlation to social and economic ancillary data. The ESRI ArcGIS (version 10.2) software was employed for geoprocessing and spatial data analysis and ENVI ITT VIS Exelis version 5.2. for digital image management (pre-treatment, processing, and post-classification). A schematic flowchart is illustrated in Fig. 2.

Dataset

A comprehensive database of various data types (containing either spatial data or non-spatial) was put together within the WADIS-MAR project, having homogeneous geometries and projections (NRD WADIS-MAR 2011; NRD WADIS-MAR 2012; NRD WADIS-MAR Project 2012). For easiness of interrogation, manipulation, overlay, and geoprocessing, hard-copy information was digitalized and stored within a database in a GIS environment, comprising agricultural calendars, pedological surveys, and well reports, as well as topographical maps, geological maps, and aerial photographs Arras et al. 2017. These consisted of the support data used for the first phase of analysis and LCLU mapping through visual interpretation.

Most of the data were made available by the WADIS-MAR local partners such as the National Agency of Hydraulic Resources of Algeria (ANRH), the Technical Institute of Development of the Sahara Agronomy (ITDAS), Arid Regions Institute (IRA), and the *Observatoire du Sahara et du Sahel* (OSS). Google Earth and its community-based ground truth data was also used as ancillary information and, partially, for the validation of the classified images (in the case of Biskra area).

In addition to this, field data were collected in both areas, though at different extents and with different procedures. The visual interpretation phase allowed us to correctly and efficiently plan the field campaigns in both areas. Cartographic material was generated containing daily itineraries and doubt points to be verified. In the Biskra area, the WADIS MAR project Algerian partners eventually performed the field survey. In the Oum Zessar area, the field campaign was conducted personally, from April to July 2014, according to a strict protocol. These observations served as ground truth data for the adjustment of the previously interpreted LCLU maps and as field data on salt-affected areas and sand encroachment areas.

The results of the field campaign in the Oum Zessar area consist of a ready-to-use geodatabase of 400 observation points with attached geotagged photographs and attributes obtained partly from land-cover sheets and attributes recorded onsite in ArcPAD GIS software on Mobile

Fig. 2 Methodological flowchart

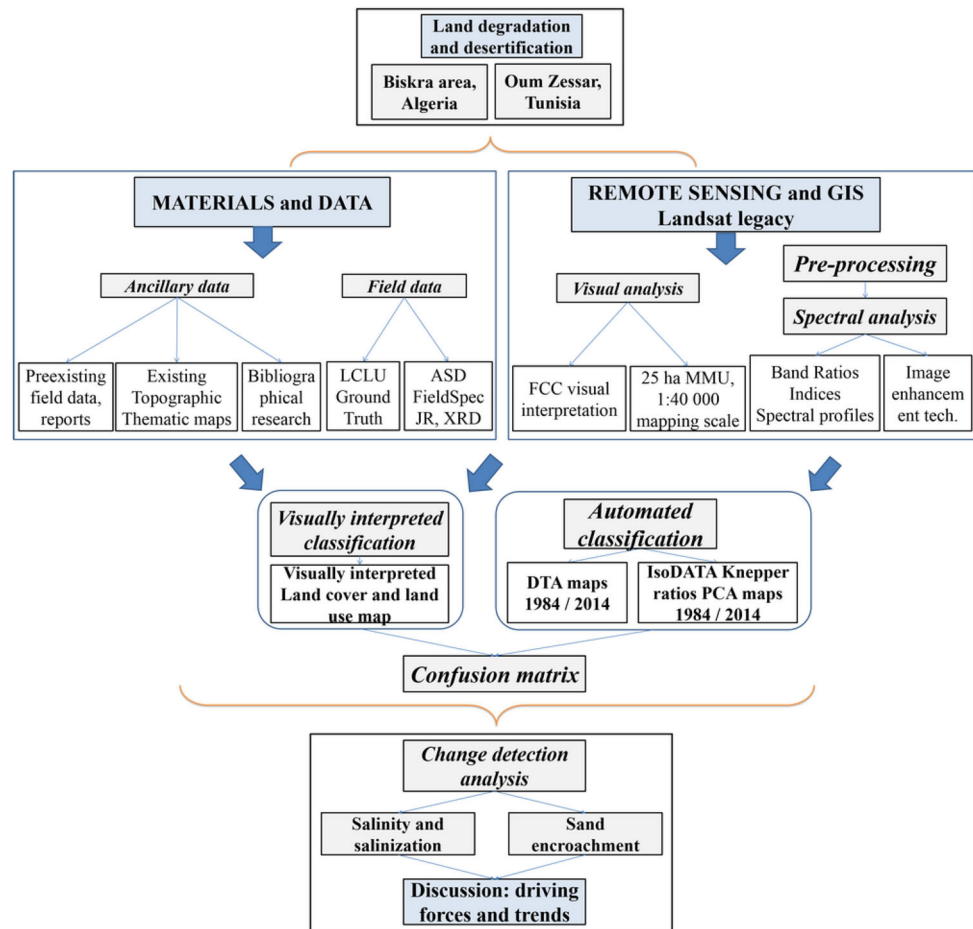


Table 1 Landsat scenes used for Biskra area and climate data

Landsat	WRS path	WRS row	Year	Date	<i>T</i>	<i>TM</i>	<i>Tm</i>	<i>SLP</i>	<i>H</i>	<i>PP</i>	<i>VV</i>	<i>V</i>	<i>VM</i>
LT5	194	36	1984	2 Sept	29.6	36.2	23.4	1017.2	29	0	13.7	10.2	25.9
LC8	194	36	2015	7 Aug	35.8	43	29	1010.2	28	0	11.6	9.6	22.2

Climatic data legend: *T* average temperature (°C), *TM* maximum temperature (°C), *Tm* minimum temperature (°C), *SLP* atmospheric pressure at sea level (hPa), *H* average relative humidity (%), *PP* total rainfall and/or snowmelt (mm), *VV* average visibility (km), *V* mean wind speed (km/h), *VM* maximum sustained wind speed (km/h) (Tutiempo Network)

Table 2 Landsat scenes used for Oum Zessar area and climate data

Landsat	WRS path	WRS row	Year	Date	<i>T</i>	<i>TM</i>	<i>Tm</i>	<i>SLP</i>	<i>H</i>	<i>PP</i>	<i>VV</i>	<i>V</i>	<i>VM</i>
LT5	190	037	1984	18 Jun	28.3	34.5	17.7	1017.3	37	0	8	15.6	25.9
LT5	191	037	1984	25 Jun	29	34.4	21.3	1015.1	49	0	8	19.3	25.9
LC8	190	037	2014	21 Jun	28.6	32.8	21.6	1013	68	0	23	11.9	18.3
LC8	191	037	2014	28 Jun	30.6	36	20.8	1017.7	47	0	24.9	9.6	14.8

Climatic data legend: *T* average temperature (°C), *TM* maximum temperature (°C), *Tm* minimum temperature (°C), *SLP* atmospheric pressure at sea level (hPa), *H* average relative humidity (%), *PP* total rainfall and/or snowmelt (mm), *VV* average visibility (km), *V* mean wind speed (km/h), *VM* maximum sustained wind speed (km/h) (Tutiempo Network)

Mapper GPS. A part of these points were also used as training data for further supervised classification and, the other part, for validation. In the Biskra area, 46 field points were described and photographed.

The Landsat satellite imagery (courtesy of USGS, earthexplorer.usgs.gov) was downloaded and selected discarding exceptionally humid years and considering only the scenes with less than 10% cloud coverage. Climate data were taken into consideration when choosing the imagery acquired during the dry season or at the end of it, as it has been reported to be the most suitable period of year for remote sensing salinity mapping (Elnaggar and Noller 2010). Scenes starting from 1984 to 2015 were employed in the analysis of the two study areas (Tables 1, 2). It must be mentioned that in the case of Oum Zessar area, two scenes were needed for the full coverage of the study area, so the closest dates as possible were chosen for the mosaic construction of each year (with color balancing).

Mapping methods

Visual interpretation

Visual interpretation is still one of the most widely used methods for identifying and classifying spatial features in a digital image. The photo-interpretation phase allowed us to identify and delineate 37 land-cover and land-use classes. Since base cartographic data of the two study areas were limited or outdated (partially dating from the 1960s, in the case of Biskra area) as well as limited in spatial coverage, this first phase was indispensable for updating pre-existing maps or even to create new ones. The creation of such detailed land cover/use maps was indispensable for the holistic knowledge and acquaintance with the study area. The LCLU maps also served as support for the following phases of the study. In addition, it allowed us to properly plan the field survey in both areas.

Their quality and validity are confirmed (Elnaggar and Noller 2010) through the use of acknowledged methodology (ETC/LC and Agency 1999; Melis and Piloni 2011; Büttner et al. 2000; Feranec and Otahel 2000; Jaffrain and EEA 2011; Melis (2012)), a large set of ancillary data, a mapping scale of 1:40,000, and a minimum mapping unit of 25 hectares (MMU). Integrating also vast ancillary data, including geomorphological insights (Dessi et al. 2008; Marini et al. 2008), we managed to delineate and define classes using objective criteria of a set of seven variables (precision of contours, color/hue, size, texture, structure, spatial distribution, and location) (ETC/LC and Agency 1999) and interpretation keys. This procedure allowed us to define and describe

the identified classes and define a customized LCLU nomenclature, adapted to the local context with a detail up to the 4th level of nomenclature equivalent to CORINE land cover, CORINE outside Europe (Sarti and ESA Earth Observation 2012) and AFRICOVER 2000.

Automated classification methods

Pre-processing

For both areas, level L1T products were radiometrically calibrated in order to obtain the top of atmosphere reflectance and atmospherically corrected by applying Dark Object Subtraction, thus obtaining surface reflectance. The information contained in the metadata of each scene was used in order to understand the level of product pre-processing undergone by the provider. Since these products were of L1T level, meaning that their provider pre-processing employed ground control points and relief models, geometric correction was not performed (Hamid Reza and Majid Shadman 2012).

The relevance of applying topographic correction was determined through an assessment of its effects when applied in arid regions such as our study areas, where land features are very reflective and the thresholds for their separation are very sensitive. Thus, this type of correction was not performed, since the state-of-art literature reported that topographic correction in desert areas are prone to over-correct values in plain areas and lose valuable information (Vanonckelen et al. 2014).

Decision tree classifier design

A complex spectral analysis was undergone in order to determine optimal data for each decision node. Several vegetation, water, and mineral indices were reviewed and applied, choosing the relevant ones reported as successful saline areas delineation (Khan et al. 2005; Immordino and Melis 2008; FAO 2009; Mulder et al. 2011; Hamid Reza and Majid Shadman 2012; Allbed and Kumar 2013) and sandy ones (Sadiq and Howari 2009; Food And Agriculture Organization of the United Nations 2010; Hadeel et al. 2011; Pandey et al. 2013; Bachir et al. 2013; Ouerchefani et al. 2013; Boulghobra 2016), respectively, in similar environmental and bio-geographical areas. The outcomes of these tests showed discrepancies in terms of correct delineation of features and accuracy of class assignment.

Nonparametric classifiers have frequently been found to yield higher classification accuracies than parametric classifiers because of their ability to cope with non-normal distributions and intra-class variation found in a variety of spectral data sets. Decision tree classifiers can perform automatic feature selection and complexity reduction,

while the tree structure gives easily understandable and interpretable information regarding the predictive or generalization ability of the data. Other advantages regard the lack of any assumptions concerning the frequency distributions of the data in each of the classes, flexibility, and ability to handle non-linear relationships between features and classes (Pal and Mather 2003; Rogan et al. 2004; Otukey and Blaschke 2010; Pal 2012).

Various types of data can be used as decision nodes, but in this study, we use specific band operations and indices. In order to construct valid indices, the bands that were highly uncorrelated (highest covariance), were used for band operations as they provided less redundant data and maximum of information content. The maximum content of information was obtained from a combination of bands that have higher covariance among them and the higher the standard deviation is, the more information content is derived from composite bands. In order to identify optimum bands for indices construction, the existing literature also proposes methods like Optimum Index Factor (OIF) or correlation analysis between measured spectral reflectance and satellite data (Yu et al. 2010; Sidike et al. 2014). In this study, this phase was undergone through a complex spectral analysis for all scenes of both areas. This involved 2D scatter plots, vertical and horizontal spectral profiles assessment, band transformation techniques with emphasis on image spectral enhancement, among the other types (spatial and radiometric).

Principal component analysis of the Knepper composite

The principal components were extracted from Knepper composites (Langford 2015). This gave us the input for understanding to what degree Knepper PC can spectrally distinguish the features of interest, namely the mineral components and vegetation types and to assess its prospective as a simple user-independent approach of fast classification, as an auxiliary to decision tree classifier, which is highly dependent on how thresholds are calculated and requires much computational labor for the determination of rules.

The IsoData classification was applied to the principal components extracted from the Knepper ratios (Langford 2015).

IsoData of Knepper ratios' PC resulting maps are compared with field data, the DTA results, and with the visually interpreted LCLU maps, and assessed for error assessment through the application of the confusion matrix.

Results and discussions

Visual interpretation LCLU mapping

In the Biskra area, the interpretation of the June 2011 Landsat scene resulted in 37 feature classes, employing the

data described in the previous sections, given the difficulty to undertake ground verification. For the Oum Zessar area, the 36 classes were delineated based on the visual interpretation of Landsat 8 images of 17 May 2013, path 190, row 37 and 24 May 2013, path 191, row 37, combined with ancillary data and the ground truth data described in the previous section. The resulting maps were validated using ground truth data in both areas, having an accuracy of 89 and 97%, in the Biskra area and Oum Zessar area, respectively.

DT classifier

The complex spectral analysis resulted in identifying the best band ratios and indices were determined through series and scalar band mathematical operations (sum, subtraction, multiplication, division, square root, exponent) in order to discriminate features of interest with the highest possible accuracy. For instance, exponential or square root functions were used to force the emphasis of extreme values, helping in delineating high or moderate saline areas (Allbed and Kumar 2013; Allbed et al. 2014).

For example, in the case of highly saline areas class extraction, Landsat visible bands of blue, green, and red information are usually put together, as they present high correlation, in order to enhance the "brightness" features. They are subsequently divided by band SWIR2, which presented the lowest reflectance values of salt features, hence high covariance with the three aforementioned. The resulting indices are thus expressed as: $\sqrt{((b1^2) + (b2^2) + (b3^2))/b7}$ or $(b1 + b2 + b3)/b7$, Salt Minerals Index and Hue Salinity Index, respectively.

Image statistics were used in order to calculate each node's threshold, considering mean and standard deviation values of each spectral index image. In order to delineate each feature of interest, regions of interest (ROIs) were created either from 2D scatter plots or through direct delineation on images and consequently statistics were extracted from each band.

Out of a total of 11 indices employed in the decision tree classifier (Table 3), five new indices were constructed by us for this particular type of study, through broad spectral analysis, band transformation techniques, image statistics, and expert-knowledge (Rao et al. 2006; Afrasinei et al. 2012b; Matthew 2012; Srimani and Prasad 2012).

The DT used for Oum Zessar area consisted of eight indices (Table 4), two of which are proposed within this study. All the indices were constructed differently for each area, depending on the spectral and biophysical-geographic particularities. The choice of the indices also depended on the features of interest to be extracted: in Biskra area, salt-affected areas had priority, followed by the main land

Table 3 DT nodes and thresholds, Biskra study site, Algeria (decision nodes)

Decision nodes	Node expressions	Band operations
NDVI	$b1 \text{ GE } 0.240$	$(\text{NIR} - \text{R})/(\text{NIR} + \text{R})$
NDWI	$b2 \text{ GE } 0.010$	$(\text{NIR} - \text{SWIR1})/(\text{NIR} + \text{SWIR1})$
NDWI USGS	$b3 \text{ GE } -0.390$	$(\text{R} - \text{NIR})/(\text{R} + \text{NIR})$
WR	$b4 \text{ GE } 1.01$	R/NIR
SMI ^a	$b5 \text{ GE } 0.740$	$\text{sqrt}(((\text{B}^2) + (\text{G}^2) + (\text{R}^2))/\text{SWIR2})$
MI ^a	$b6 \text{ GE } 0.0280$	$(\text{B} \times \text{G} \times \text{R})/\text{NIR}$
IRI_SWIR1 ^a	$b7 \text{ GE } 0.880$	$\text{sqrt}(((\text{NIR}^2) + (\text{SWIR2}^2))/\text{SWIR1})$
IRI_NIR ^a	$b8 \text{ GE } 1.70$	$\text{sqrt}(((\text{SWIR1}^2) + (\text{SWIR2}^2))/(\text{NIR}^2))$
S2	$b9 \text{ LE } -0.320$	$(\text{B} - \text{R})/(\text{B} + \text{R})$
HIS ^a	$b10 \text{ GE } 1.740$	$(\text{B} + \text{G} + \text{R})/\text{SWIR2}$
1/5	$b11 \text{ GE } 0.220$	$\text{B}/\text{SWIR1}$

^a Indices proposed in this study

Table 4 DT nodes and thresholds, Oum Zessar area, Tunisia (decision nodes)

Decision nodes	Node expressions	Band operations
NDVI	$b1 \text{ GT } 0.1450$	$(\text{NIR} - \text{R})/(\text{NIR} + \text{R})$
Ratio 5/2	$b3 \text{ GT } 4.20$	(NIR/B)
Diff 5 - 2	$b5 \text{ GT } 0.370$	$(\text{NIR} - \text{B})$
Ratio 6/3	$b7 \text{ GT } 3.10$	$(\text{SWIR1} - \text{G})$
Diff NDVI - NDWI	$b8 \text{ GT } 0.260$	$((\text{NIR} - \text{R})/(\text{NIR} + \text{R})) - ((\text{NIR} - \text{SWIR1})/(\text{NIR} + \text{SWIR1}))$
MMI ^a	$b4 \text{ GT } 0.60$	$(\text{sqrt}(\text{R} \times \text{R}) + (\text{SWIR1} \times \text{SWIR1}))$
Modif SI ^a	$b6 \text{ GT } 0.450$	$(\text{sqrt}(\text{B} \times \text{B}) + (\text{NIR} \times \text{NIR}))$
NDWI	$b2 \text{ GT } -0.050$	$(\text{NIR} - \text{SWIR1})/(\text{NIR} + \text{SWIR1})$

^a Indices proposed in this study

cover types, whereas in Oum Zessar area, the sandy ones were given priority, followed by the saline ones and eventually five other land-cover classes. In fact, the hierarchical input order of the indices within each tree was based on these priorities.

The normalized vegetation index, two water indices, existing and new salinity indices as well as simple band ratios were employed in the DT classifier and the final map was obtained. The choice of the indices or band operations that were derived through the previous spectral analysis have proven to give optimal results (Melis et al. 2013). The threshold values of the decision nodes were derived from each index image statistics, considering mean values and standard deviation. The DT classifier was applied for 1984 and 2015 images in the case of Biskra area and for 1984 and 2014 for the Oum Zessar area. The example of Biskra area is presented in Figs. 3 and 4, and the Oum Zessar one, in Figs. 5 and 6. The DT components and class description were tailored for each study site considering their particular bio-physical characteristics, bearing in mind especially their specific lithology and the main types of vegetation cover that can be spectrally distinguished among themselves, respectively. The validation of the DT maps showed

an overall accuracy of 81% in the case of Biskra and 89% in the case of Oum Zessar.

IsoData classifier of Knepper composite PC

Principal components analysis indicated that the information regarding the abundant salt minerals were found within the third component in both years' images in the case of Biskra area. The highest amount of irredundant data of the three input images (namely the Knepper ratios) was related to sand minerals, emphasized by the first principal component. Clay minerals were emphasized by the second component, usually overlaying alluvial fans areas where sandy, loamy, or clayey soils are usually present.

Consequently, the resulting PC bands were further classified using unsupervised classification, IsoData in ENVI 5.2. ITT VIS Exelis Boulder, CO, applied with 100 iterations and a 2% threshold in order to obtain a clear delineation of saline areas and sandy areas. The seven major classes were not delineated correctly using IsoData classification since it presented misclassification issues in both areas and it has given an overall accuracy inferior to 60%. Therefore, only the "saline soil" and "moderately

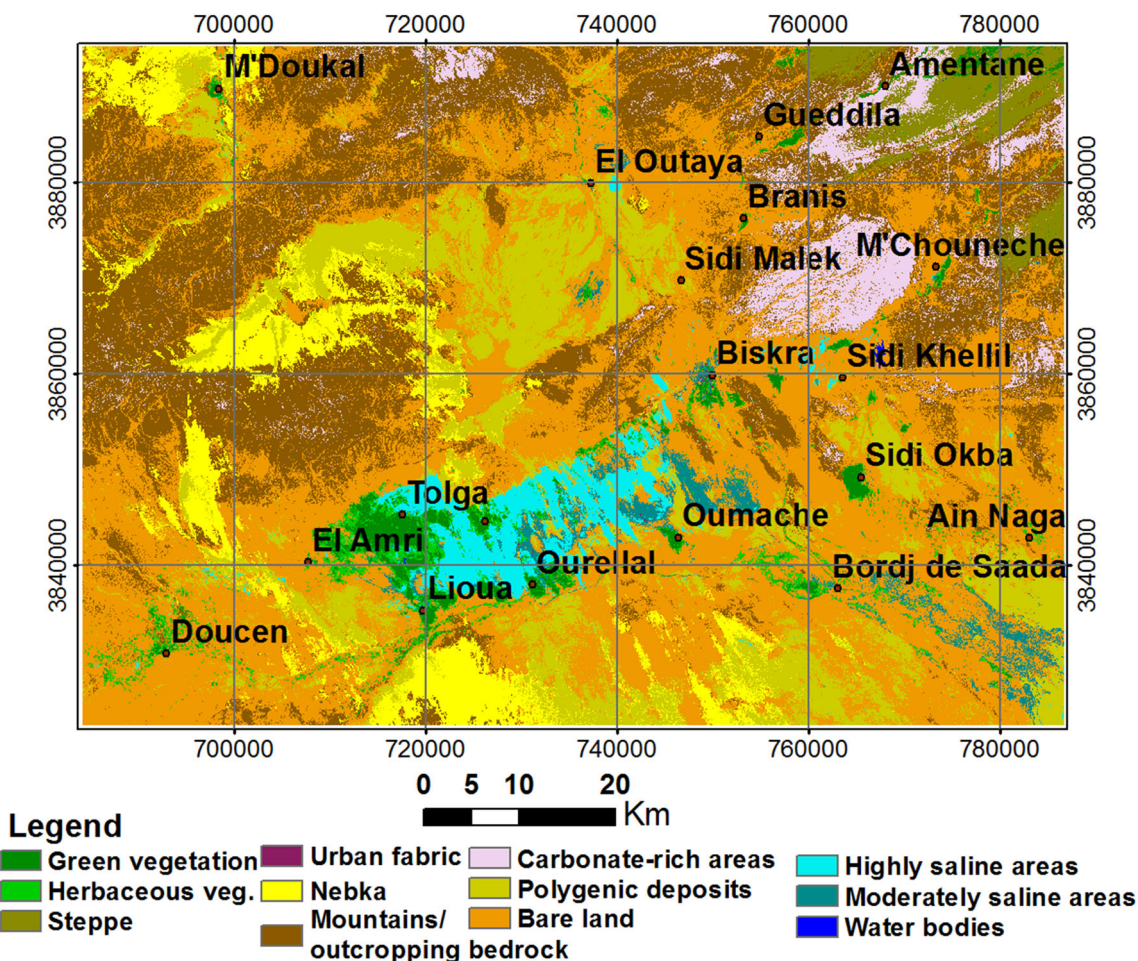


Fig. 3 Decision tree applied to 1984 Landsat scene, Biskra area, Algeria

saline areas” classes have been employed for the for change detection analysis. In the Oum Zessar area, the third principal component contained the sandy areas information and good results have also been obtained on the spectral distinction between the aeolian sand West of Dahar and the inner-plain one. IsoData has been applied on the three resulting components, but with several issues of misclassification.

Discussion

Soil salinity mapping issues

The observations that were made on the Biskra satellite images during the pre-classification phase, related to the analysis of the features of interest from the spectral point of view, revealed that the main elements that generally influence the reflectance of salty soils are the content and mineralogical typology of salts. Added to these, the physical properties are also important, such as moisture content, surface roughness, impurities, or color.

The spectral signature is influenced by the mineralogy of the chloride, carbonate, or sulfate salts, hence elementary anion groups (carbonate, sulfate, hydroxyl, and hydroxide). These trigger the behavior of tones, either exciting them or favoring combinations, which are related to the internal vibration modes translated into the presence/absence of absorption features (Metternicht and Zinck 2008; Muller and van Niekerk 2016b). Given this premise, it can be explained why we encountered difficulties in correctly identifying the saline features, even though it must be mentioned that the *highly saline areas* class has presented the highest degree of misclassification because of spectral similarity to areas that have a strong carbonate component and implicitly outcropping limestone. Various tests were conducted on the images applying salinity indices indicated by the literature (Abbas et al. 2013; Allbed et al. 2014; Masoud 2014), but no substantial outcomes were achieved. This is argued by the fact that clayey soils, silty soils, impervious surfaces, bare rock and land, as well as carbonate-rich areas presented high similarity to saline areas so as to be classified altogether in one unique class.

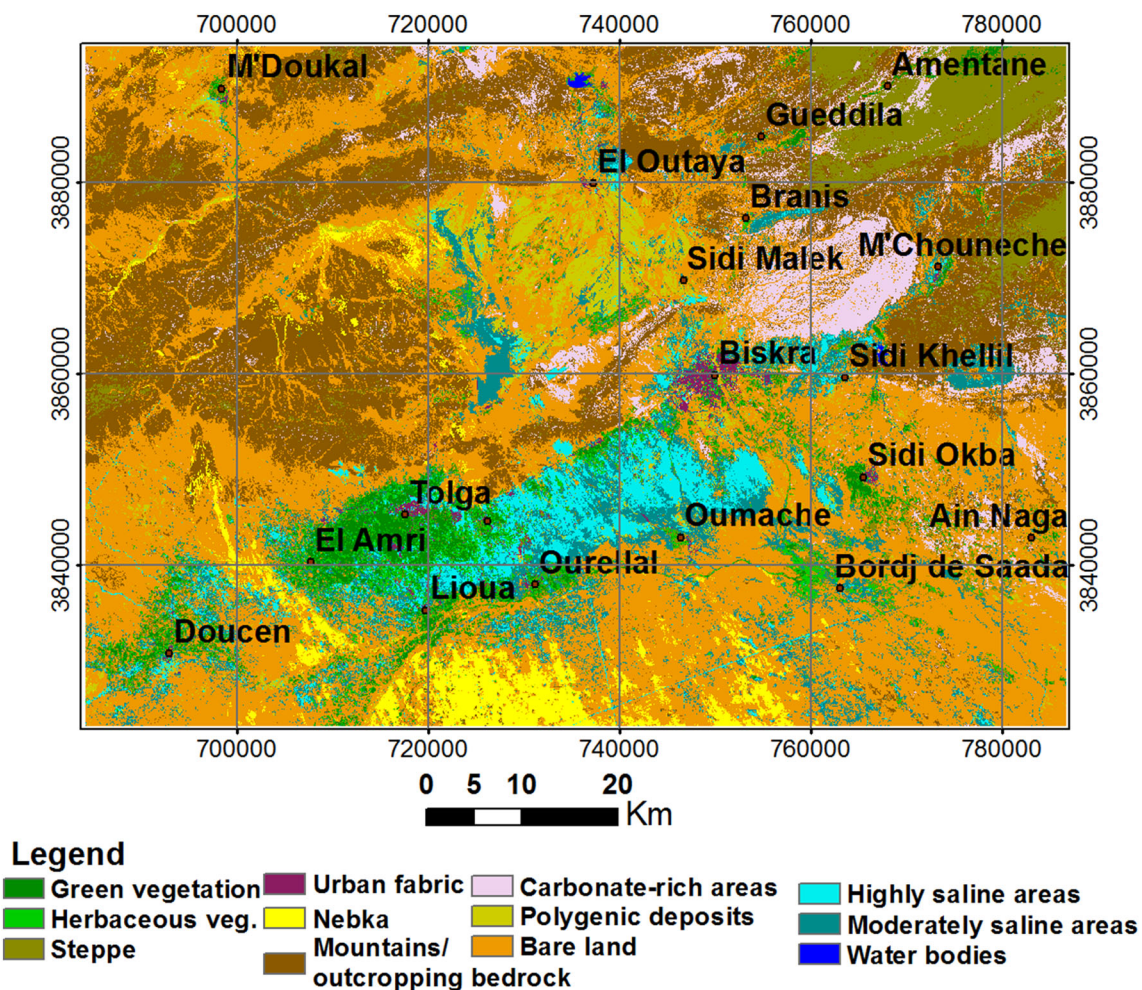


Fig. 4 Decision tree applied to 2015 Landsat scene, Biskra area, Algeria

We managed to minimize these issues, and the DT classifier showed agreeable results and an overall accuracy of over 85%. However, it must be mentioned, as an overall observation, that from both spectral analysis and classification phases we can determine that common drylands features that are highly reflective may present high levels of similarity to those of areas with high salt concentration. Such common drylands features are braided stream beds, eroded surfaces with skeletal soils, and non-saline silt-rich structural crusts, as previously stated in the literature (Metternicht and Zinck 2008).

Change detection and driving factors

In the Biskra study area, the geological setting consists of mainly limestone, alluvial deposits, and other sedimentary deposits with a strong component of evaporite minerals (mainly gypsum and halite). These geological characteristics give an a priori favorable background for the leaching and mobility of soluble salts, mainly Na chlorides and Ca

sulfates (no sodic or alkaline soils issue) and their deposition in lower topographies. Secondary salinization mostly occurs in lowland areas, where groundwater frequently rises up through the soil profile through seepage (Yahiaoui et al. 2015). Most soils in this region are composed of gypseous soil, or gypsum ($\text{CaSO}_4 \cdot 2\text{H}_2\text{O}$), which is common in geologic materials, groundwater, and surface area (Aly et al. 2016).

Previous research showed the effectiveness of employing hybrid approaches for soil mapping, and particularly gypseous soils. In this sense, several studies used remote sensing, field, and laboratory data in order to map gypsum content of soil (Mostephaoui et al. 2013) or assess the diachronic evolution of wetlands in desert areas, comparing maximum likelihood classification, support vector machines (SVM), spectral angle mapper, and neural network (Medjani et al. 2015). In this latter case, the SVM presented the highest accuracy for the identification of nine classes of humid zones (five classes) and mineral surfaces (four classes). In both cases, they obtained good results

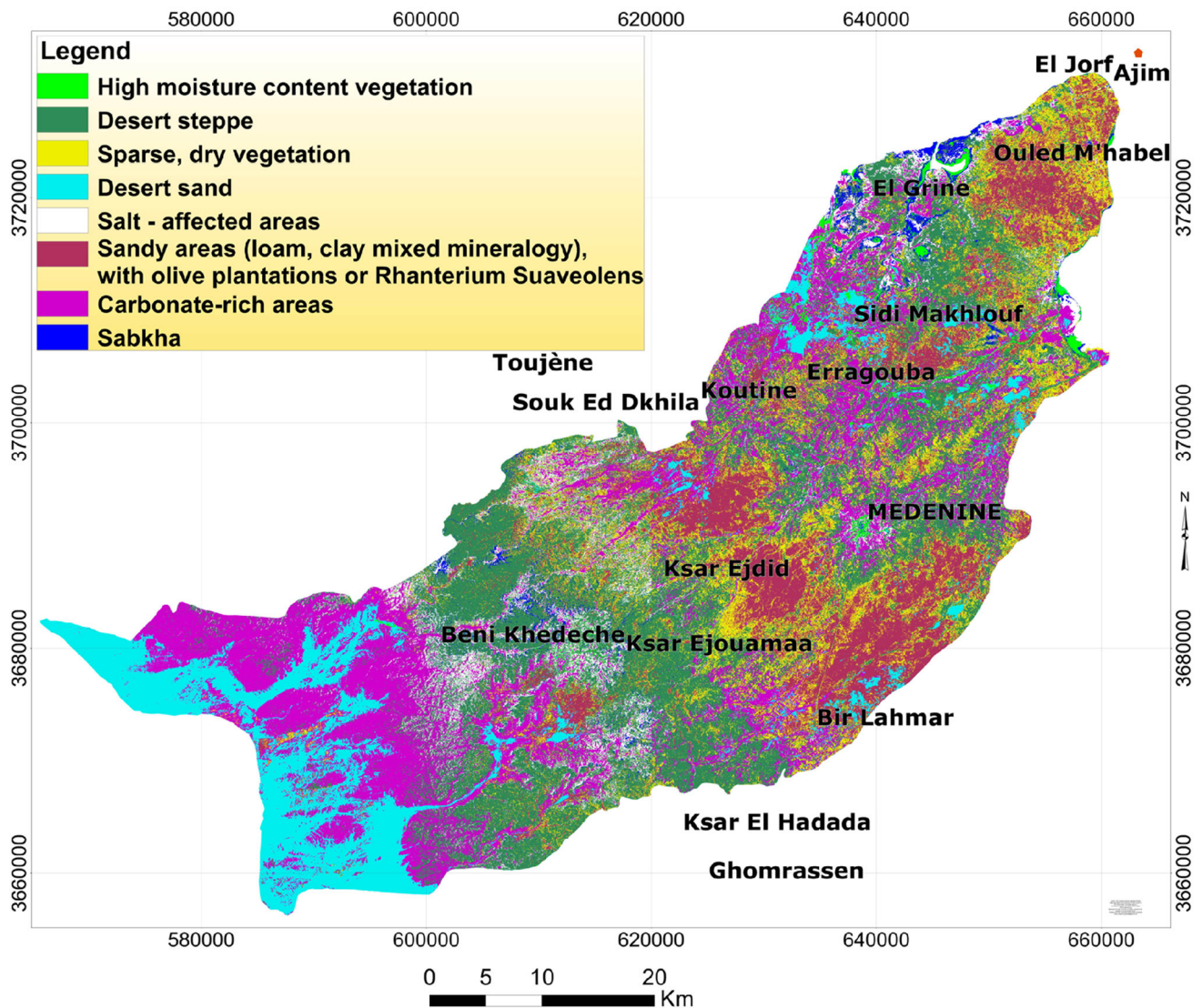


Fig. 5 DT classification of the 1984 Landsat mosaic image, Oum Zessar area, Tunisia

employing the chosen methods and according to the scope of their studies. However, if aiming at a high number of different land-cover classes, in such areas, more flexible and controllable nonparametric classifiers should be considered, such as multi-stage decision trees (Li 2014; Sidike et al. 2014).

Considering driving factors of secondary salinization of soils, it is important to highlight the contribution of the anthropic factors. In the Biskra area of Algeria, one of the important aspects that has emerged from the diachronic series analyses is that the expansion of open-field and industrial agriculture practices in the last three decades has led to (and continues to) contribute to a secondary salinization of soils. The field and pre-existing literature data confirm that the intensive irrigation uses high-salinity groundwater (mainly exploited from the highly productive and superficial

aquifers, of an average salinity of 2–4 g/l). In fact, the change detection analysis shows that where the irrigated crops expanded from 1984 to 2015, patches of salinized soil appeared in the 2015 image. In the Occidental Zab, the increase in salinized soils corresponds to the expansion of phoeniculture and market gardening (often greenhouse). In the Oriental Zab, the large-scale industrial agriculture, which also required a large number of deep wells (given the 200–300 m depth of the exploitable groundwater), has caused sporadic local appearance of small patches of salinized surfaces all along the lower slope of the alluvial fan area, patches that were not present in the 1980s and started to appear only after 2007. In accordance, change detection statistics of the 1984 and 2015 years (Fig. 7) have shown an increase of approx. 76% of the surface of salt-affected areas, including “moderately saline areas” class, mainly in the

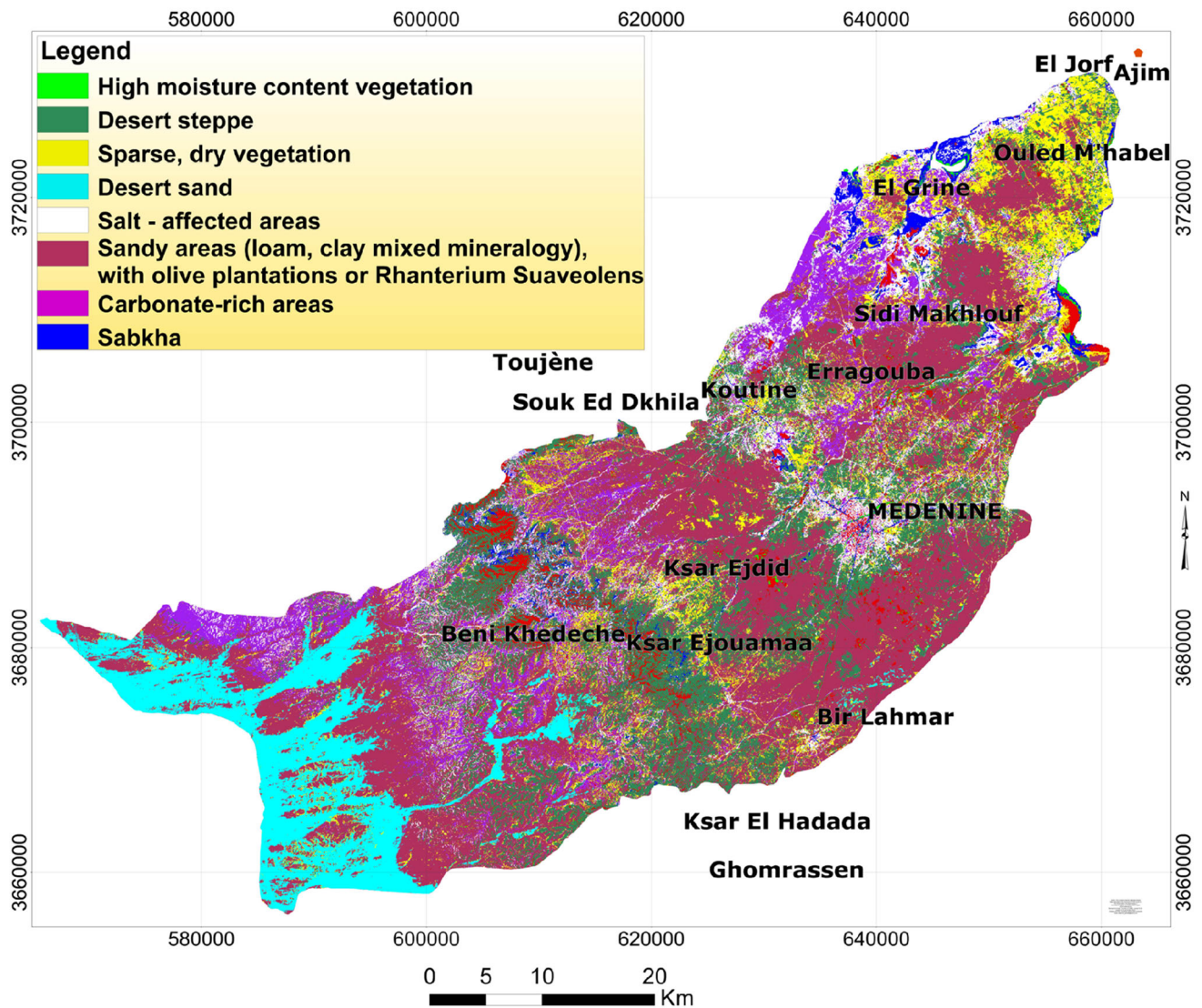


Fig. 6 DT classification of the 2014 Landsat mosaic image, Oum Zessar area, Tunisia

disfavor of steppe vegetation (18%), polygenic deposits (2%), green vegetation (around 16%), and other small percentages of other classes.

In the Oum Zessar area, the *aeolian sand* class presented an increase of 10, 13% and the desert one, of 10, 44%, between 1984 and 2014. The land-cover classes' changes are presented in Fig. 8. However, the PCA of the Knepper composites between the same years have shown an increase of 21% of *aeolian sand* class and 19% of *desert sand* class, as resulted from the change detection statistics. The *desert sand* class had presented problems of spectral confusion with another feature (possibly saline areas in the western extremity of the image), as shown from comparison to IsoData of Knepper PCA and ground truth data, thus the index employed to extract it needs further revision. In the DT classification map, the *desert sand* class was overestimated. Thus, we have reached our goal of

separating *desert sand* class from the inner plain aeolian sand, but we cannot appreciate the change between the two dates, as the DT classification needs further revision. It is also important to mention that the sparse vegetation on sand-encroached areas, mainly psammophyte species, have decreased by 40%, which can be argued by the fact that in the past decades the rainfed agriculture, and especially olive plantations, overlay mostly to the inner-plain sandy areas.

The most important aspect obtained from this analysis was the net separation between inner-plain aeolian sandy areas and the desert ones along paleo-valleys that converge towards the Great Oriental Erg. Both classification methods have shown good separability between the two classes for both years in discussion.

The analyzed data also indicated that the salt-affected areas have increased by 41.45% and the classification maps

Fig. 7 Variations in land cover classes from 1984 to 2015, Biskra area

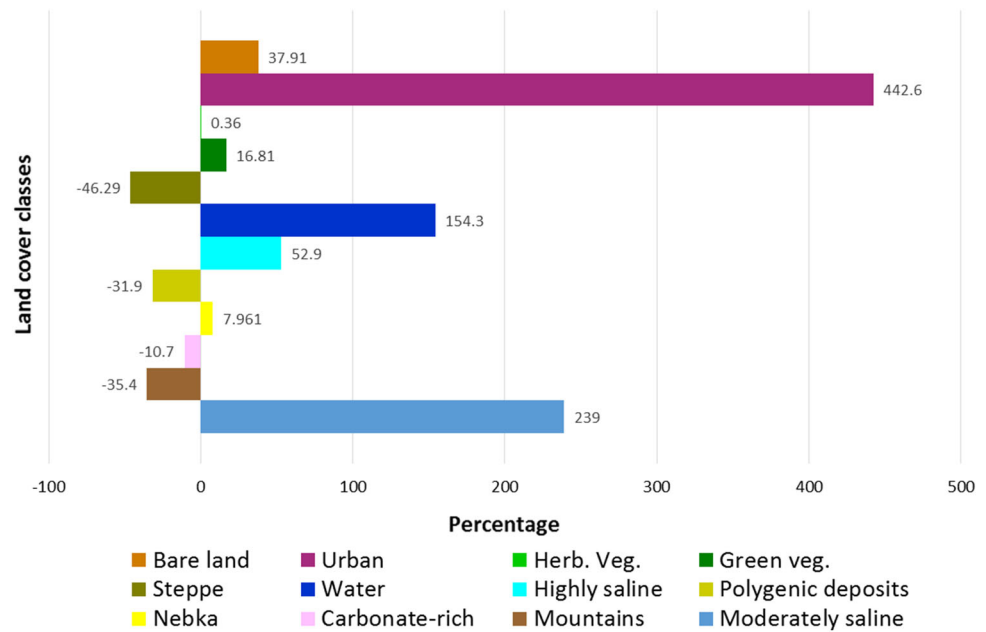
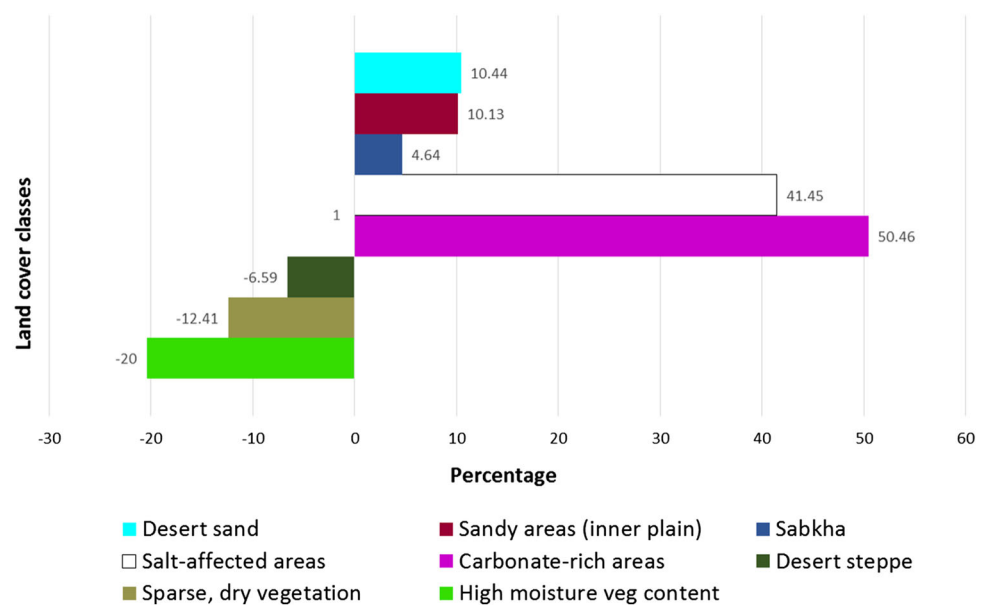


Fig. 8 Variations in landcover classes from 1984 to 2014, Oum Zessar area



and field observations show that these areas are not located only within or nearby the sebkha areas. These are also spread within the Jeffara Plain, especially where irrigated perimeters are, mostly along the Koutine-Medenine area or west and south-west of Medenine. This is may be argued through the presence of the faults' system in the area (Koutine-Medenine main one) which favors an intense exploitation of high-salinity groundwater (Chihi et al. 2015) used for irrigation, among other usages. The presence of many wells along this alignment induces a rather high concentration of irrigated fields in this area. Also according to Farid et al. 2013, this may be related to the urban and industrial development and the expansion of

irrigated agriculture, which led to an increase and even over-exploitation of the aquifers of the Jeffara Plain, which has seriously degraded groundwater quality. Intensive exploitation of the aquifer, seawater intrusion in the coastal area, and climate aridity caused a decrease in piezometric level and an increase in salinity.

Conclusions

Based on a vast bibliography, this work combines and proposes a specific workflow for thematic mapping, indices construction and classification built-up, and change

detection analysis. The employment of two different classification approaches, of either visual interpretation or automated, provided invaluable support for identification and correct delineation of features of interest. The customized decision tree classifier has proven to be more flexible and adequate for the extraction of two types of saline areas, two types of sandy areas and major land cover types, as it allows multi-source information and higher user control, with an overall accuracy of more than 85% in both areas. Seven new indices employed in the decision tree classifiers are proposed and validated, including a salinity index (SMI) for the extraction of highly saline areas. The customized classification methods can be repeated both in space and in time. The assessment and definition of appropriate spectral indices, as well as the construction of a customized decision tree classifier according to study scope, are also repeatable.

The results showed that the secondary salinization of soils is an ongoing process in the Biskra area of Algeria and the main driving factors are related to human activities, namely the intensification of agriculture, through the enlargement of date palm plantation and market gardening fields in the Occidental Zab and the expansion of open-field and large-scale industrial agriculture practices in the Oriental Zab. In the Oum Zessar study area in Tunisia, the analyses show a substantial change in several components of the environment since the 1980s, related to increased anthropic pressure, settlement, and agricultural policies and national development strategies. One of the concerning aspects that emerged from this study is that the Jeffara Plain is more affected by sand encroachment over the last decade, adding also changes in several other classes of land cover. The anthropic factors may have substantial contribution to the genesis of sand material and autochthone sand-encroachment process of the plain of Jeffara-Medenine area (east of Dahar area).

This paper addresses the very important issue of accurately mapping and monitoring land degradation due to salinization and sand encroachment, respectively. They both are highly dynamic processes and their mapping and monitoring are very important to establish sustainable strategies at local level as well as regional level. Finally, the identification of driving factors, which lead to land-cover and/or land-use change and land degradation, are very useful for decision-makers and stakeholders.

Acknowledgments This study was developed within the frame of the doctoral research (2013-2016) of Gabriela Mihaela Afrasinei, financed by the Italian Ministry of Education, Universities and Research (MIUR), in “Soil preservation, environmental vulnerability, and hydrogeological protection” of the PhD school in Environmental and Land Sciences and Engineering, University of Cagliari (Italy). This work is partly supported and developed within the Water

Harvesting and Agricultural Techniques in Dry Lands: an Integrated and Sustainable Model in MAghreb Regions (WADIS-MAR) Demonstration Project, funded by the EU Commission through the SWIM Programme (www.wadismar.eu). We wish to acknowledge the WADIS-MAR project and its team, the Desertification Research Centre (NRD) team of the University of Sassari, and the TeleGIS Laboratory team of the University of Cagliari (Italy) for the scientific and financial support, and the possibility of conducting the current research. We also wish to thank the *Institut des Regions Arides* of Medenine, Tunisia and Algerian WADIS-MAR partners, for the provided data and support and also the Spatial Analysis Laboratory of Wollongong University NSW, Australia, for the undertaken research training programme. We also acknowledge the contribution given by the fellow researchers and professors of the Chemical and Geological Department of the University of Cagliari, among which are Prof. Andrea Vacca and Dr. Marco Pistis.

Compliance with ethical standards

Conflict of interest On behalf of all authors, the corresponding author states that there are no conflicts of interest.

References

- Abbas A, Khan S, Hussain N, Hanjra MA, Akbar S (2013) Characterizing soil salinity in irrigated agriculture using a remote sensing approach. *Phys Chem Earth* 55–57:43–52. doi:[10.1016/j.pce.2010.12.004](https://doi.org/10.1016/j.pce.2010.12.004)
- Afrasinei GM (2016) Study of land degradation and desertification dynamics in North Africa areas using remote sensing techniques. doi:[10.13140/RG.2.1.2412.6327](https://doi.org/10.13140/RG.2.1.2412.6327)
- Afrasinei GM, Melis MT, Buttau C, Bradd JM, Arras C, Ghiglieri G (2015a) Diachronic analysis of salt-affected areas using remote sensing techniques: the case study of Biskra area, Algeria. *Proc SPIE* 9644:96441D. doi:[10.1117/12.2194998](https://doi.org/10.1117/12.2194998)
- Afrasinei GM, Melis MT, Frau F, Demurtas V, Buttau C, Arras C, Ghiglieri G (2015b) Spectral characterization methodology of saline and sand encroachment areas using proximal sensing e remote sensing in Tunisia. *ASITA* 19, p 11–18. <http://atti.asita.it/ASITA2015/Pdf/1-322.pdf>. Accessed 17 June 2017
- Afrasinei GM, Melis MT, Buttau C, Arras C, Zerrim A, Guied M, Ouessar M, Essifi B, Zaied MB, Jjali A, Jarray H, Ghiglieri G (2017a) Classification methods for detecting and evaluating changes in desertification-related features in arid and semi-arid environments. In: Ouessar et al (eds) *Water and land security in drylands*, Springer. doi: [10.1007/978-3-319-54021-4_23](https://doi.org/10.1007/978-3-319-54021-4_23)
- Afrasinei GM, Melis MT, Buttau C, Bradd JM, Arras C, Ghiglieri G (2017b) Assessment of remote sensing-based classification methods for change detection of salt-affected areas (Biskra area, Algeria). *J Appl Remote Sens* 11:16025. doi:[10.1117/1.JRS.11.016025](https://doi.org/10.1117/1.JRS.11.016025)
- Aleksandrowicz S, Turlej K, Lewiński S, Bochenek Z (2014) Change detection algorithm for the production of land cover change maps over the European Union countries. *Remote Sens* 6:5976–5994. doi:[10.3390/rs6075976](https://doi.org/10.3390/rs6075976)
- Allbed A, Kumar L (2013) Soil salinity mapping and monitoring in arid and semi-arid regions using remote sensing technology: a review. *Adv Remote Sens* 2:373–385. doi:[10.4236/ars.2013.24040](https://doi.org/10.4236/ars.2013.24040)
- Allbed A, Kumar L, Aldakheel YY (2014) Assessing soil salinity using soil salinity and vegetation indices derived from IKONOS high-spatial resolution imageries: applications in a date palm dominated region. *Geoderma* 230–231:1–8. doi:[10.1016/j.geoderma.2014.03.025](https://doi.org/10.1016/j.geoderma.2014.03.025)

- Aly AA, Al-Omran AM, Sallam AS, Al-Wabel MI, Al-Shayaa MS (2016) Vegetation cover change detection and assessment in arid environment using multi-temporal remote sensing images and ecosystem management approach. *Solid Earth Discuss*. doi:10.5194/se-2016-31
- Arras C, BabaSy M, Buttau C, Da Pelo S, Carletti A, Afrasinei GM, Ghiglieri G (2016) Preliminary results of a 3-D groundwater flow model in an arid region of NE Algeria using PMWin: the Inféro-flux phreatic aquifer (Biskra). *Rend Online Soc Geol It* 41:18–21. doi:10.3301/ROL.2016.82
- Arras C, Melis MT, Afrasinei G-M, Buttau C, Carletti A, Ghiglieri G (2017) Evaluation and validation of SRTMGL1 and ASTER GDEM2 for two Maghreb regions (Biskra, Algeria and Medenine, Tunisia). In: Ouessar M et al (eds) *Water and land security in drylands*. Springer, AG, pp 291–301
- Asfaw E, Suryabhadgavan KV, Argaw M (2016) Soil salinity modeling and mapping using remote sensing and GIS: The case of Wonji sugar cane irrigation farm, Ethiopia. *J Saudi Soc Agric Sci*. doi:10.1016/j.jssas.2016.05.003
- Avelar S, Tokarczyk P (2014) Analysis of land use and land cover change in a coastal area of Rio de Janeiro using high-resolution remotely sensed data. *J Appl Remote Sens* 8:83631. doi:10.1117/1.jrs.8.083631
- Bachir M, Essifi B, Zerrim A, Ouessar M (2013) Dynamique de l'occupation de sol à travers une classification multi-temporelle des images Landsat-5 et 7 dans le bassin versant d'Oum Zessar (Sud Tunisie). In: GEOTUNIS
- Bouaziz M, Matschullat J, Gloaguen R (2011) Improved remote sensing detection of soil salinity from a semi-arid climate in Northeast Brazil. *CR Geosci* 343:795–803. doi:10.1016/j.crte.2011.09.003
- Boulghobra N (2016) Climatic data and satellite imagery for assessing the aeolian sand deposit and barchan migration, as a major risk sources in the region of In-Salah (Central Algerian Sahara). *Arab J Geosci*. doi:10.1007/s12517-016-2491-x
- Buttau C, Funedda A, Carletti A, Ghiglieri G (2013) Studio geologico strutturale per indagini idrogeologiche dell'area compresa tra le regioni di Batna e Biskra (NE Algeria). *Rend Online Soc Geol It* 29:13–16
- Ceccarelli T (2013) Land cover data from Landsat single-date imagery: an approach integrating pixel-based and object-based classifiers. *Eur J Remote Sens*. doi:10.5721/EuJRS20134641
- Chihi H, de Marsily G, Belayouni H, Yahyaoui H (2015) Relationship between tectonic structures and hydrogeochemical compartmentalization in aquifers: example of the “Jeffara de Medenine” system, south-east Tunisia. *J Hydrol* 4:410–430. doi:10.1016/j.ejrh.2015.07.004
- Da Pelo S, Ghiglieri G, Cuzzocrea C, Carletti A, Fenza P, Arras C (2015) 3D hydrogeological modelling supported by geochemical mapping as an innovative approach for management of aquifers applied to the Nurra district. Sardinia, Italy
- Dessi F, Marini A, Melis MT (2008) HR remote sensing data for the mapping of morphodynamic units in the area of Oung El-Jemel (SW Tunisia) | telerilevamento ad alta risoluzione per il riconoscimento dei domini morfodinamici nell'area di Oung El-Jemel (Tunisia SW). *Rend Online Soc Geol It* 3:330–331
- De Waele J, Di Gregorio F, El Wartiti M, Fadli D, Follasa R, Marini A, Melis MT (2004) Geoenvironmental risk in the upper valley of the Oued Sebou (Fès, Central Morocco): a preliminary approach. *J Afr Earth Sci* 39:491–500. doi:10.1016/j.jafrearsci.2004.07.015
- Dhaou H, Belghith A (2009) Le zonage agroécologique, un outil nécessaire de suivi-evaluation des milieux sensibles
- Duan HC, Wang T, Xue X, Liu SL, Guo J (2014) Dynamics of aeolian desertification and its driving forces in the Horqin Sandy Land, northern China. *Environ Monit Assess* 186:6083–6096. doi:10.1007/s10661-014-3841-3
- Elnaggar AA, Noller JS (2010) Application of remote-sensing data and decision-tree analysis to mapping salt-affected soils over large areas. *Remote Sens* 2:151–165. doi:10.3390/rs2010151
- Essifi B, Ouessar M, Rabia MC (2009) Mapping long-term variability of vegetation greenness and sand dunes around watering points in the rangelands of Dahar and El Ouara (Tataouine-Tunisia) during the period 1975–2000 using remote sensing. *J Arid Land Stud* 19:319–322
- ETC/LC, Agency EE (1999) CORINE land cover. Technical guide. ETC/LC, European Environment Agency
- Eyal B-D, Graciela M, Naftaly G, Eshel M, Vladmir M, Uri B (2008) Review of remote sensing-based methods to assess soil salinity. In: *Remote sensing of soil salinization*. CRC Press, Boca Raton
- FAO (2009) Advances in the assessment and monitoring of salinization and status of biosaline agriculture. Reports of expert consultation held in Dubai, United Emirates, 26–29 November 2007, Rome
- Fares MH, Philip CG (2008) Characterization of salt-crust build-up and soil salinization in the United Arab Emirates by means of field and remote sensing techniques. In: Metternicht G, Zinck A (eds) *Remote sensing of soil salinization*. CRC Press, Boca Raton
- Farid I, Trabelsi R, Zouari K, Abid K, Ayachi M (2013) Hydrogeochemical processes affecting groundwater in an irrigated land in Central Tunisia. *Environ Sci* 68:1215–1231. doi:10.1007/s12665-012-1788-7
- Feranec J, Otahel J (2000) The 4th level corine land cover nomenclature for the phare countries. Institute of geography, Slovak academy of sciences, Bratislava, Slovak Republic. http://www2.dmu.dk/1_Viden/2_Miljoe-tilstand/3_natur/nordlam/nldocs/wsOct01T1/jferanec.pdf. Accessed 17 June 2017
- Fichera CR (2012) Land Cover classification and change-detection analysis using multi-temporal remote sensed imagery and landscape metrics. *Eur J Remote Sens*. doi:10.5721/EuJRS20124501
- Food And Agriculture Organization Of The United Nations (2010) *Fighting sand encroachment—Lessons from Mauritania*
- Fu H, Gu L, Ren R, Sun J (2014) Land salinization classification method using Landsat TM in western Jilin Province of China, p 92200U–92200U–12
- Ge X, Dong K, Luloff AE, Wang L, Xiao J, Wang S, Wang Q (2016) Correlation between landscape fragmentation and sandy desertification: a case study in Horqin Sandy Land, China. *Environ Monit Assess* 188:62. doi:10.1007/s10661-015-5039-8
- Gorji T, Tanik A, Sertel E (2015) Soil salinity prediction, monitoring and mapping using modern technologies. *Procedia Earth Planet Sci* 15:507–512. doi:10.1016/j.proeps.2015.08.062
- Graaff J de, Ouessar M (2002) Water harvesting in Mediterranean zones: an impact assessment and economic evaluation. *Proceedings from EU Wahia project final seminar in Lanzarote*
- Hadeel AS, Jabbar MT, Chen X (2011) Remote sensing and GIS application in the detection of environmental degradation indicators. *Geo-Spatial Inform Sci* 14:39–47. doi:10.1007/s11806-011-0441-z
- Hamid Reza M, Majid Shadman R (2012) Decision tree land use/ land cover change detection of khoram abad city using landsat imagery and ancillary SRTM data. *An Biol Res* 8:4045–4053
- Hanafi A, Jauffret S (2008) Are long-term vegetation dynamics useful in monitoring and assessing desertification processes in the arid steppe, southern Tunisia. *J Arid Environ* 72:557–572. doi:10.1016/j.jaridenv.2007.07.003
- Immordino EF, Melis MT (2008) Applicazione di indici spettrali a dati SPOT per lo studio delle marshlands dell'Iraq meridionale.

- In: Atti del 84° Congresso della Soc Geologica Italiana, Sassari, vol 3/2, pp 474–475
- Jan F, Tomas S, Gerard H, Gabriel J (2012) Land cover and its change in Europe. In: Remote sensing of land use and land cover. CRC Press, Boca Raton, pp 285–302
- Khan NM, Rastokuev VV, Sato Y, Shiozawa S (2005) Assessment of hydrosaline land degradation by using a simple approach of remote sensing indicators. *Agric Water Manag* 77:96–109. doi:10.1016/j.agwat.2004.09.038
- Khatelli H, Gabriels D (2000) Effect of wind direction on aeolian sand transport in southern Tunisia. *Int Agrophys* 14:291–296
- Lamchin M, Lee J-Y, Lee W-K, Lee EJ, Kim M, Lim C-H, Choi H-A, Kim S-R (2016) Assessment of land cover change and desertification using remote sensing technology in a local region of Mongolia. *Adv Space Res* 57:64–77. doi:10.1016/j.asr.2015.10.006
- Langford RL (2015) Temporal merging of remote sensing data to enhance spectral regolith, lithological and alteration patterns for regional mineral exploration. *Ore Geol Rev* 68:14–29. doi:10.1016/j.oregeorev.2015.01.005
- Li M (2014) A review of remote sensing image classification techniques: the role of spatio-contextual information. *Eur J Remote Sens*. doi:10.5721/EuJRS20144723
- Lorenz RD, Gasmi N, Radebaugh J, Barnes JW, Ori GG (2013) Dunes on planet Tatooine: observation of barchan migration at the Star Wars film set in Tunisia. *Geomorphology* 201:264–271. doi:10.1016/j.geomorph.2013.06.026
- Marconcini M, Fernandez-Prieto D, Buchholz T (2014) Targeted land-cover classification. *IEEE Trans Geosci Remote Sens* 52:4173–4193. doi:10.1109/TGRS.2013.2280150
- Marini A, Melis MT, Pitzalis A, Talbi M, Gasmi N (2008) La carta della unità geomorfologiche della regione di Medenine (Tunisia meridionale). *Mem Descr Carta Geol d'It LXXVIII*:153–168
- Masoud AA (2014) Predicting salt abundance in slightly saline soils from Landsat ETM+ imagery using spectral mixture analysis and soil spectrometry. *Geoderma* 217–218:45–56. doi:10.1016/j.geoderma.2013.10.027
- Matthew CH (2012) Classification trees and mixed pixel training data. In: Remote sensing of land use and land cover. CRC Press, Boca Raton, pp 127–136
- Medjani F, Hamdaoui O, Djidel M, Ducrot D (2015) Diachronic evolution of wetlands in a desert arid climate of the basin of Ouargla (southeastern Algeria) between 1987 and 2009 by remote sensing. *Arab J Geosci* 8:10181–10192. doi:10.1007/s12517-015-1958-5
- Melis MT (2012) Landforms and soils. In: Mediterranean mountain environments vogiatzakakis/mediterranean mountain environments, pp 65–85.
- Melis MT, Pilloni M (2011) Analysis and validation of a methodology to evaluate land cover in the mediterranean basin using multitemporal MODIS data [Analisi e validazione di una metodologia per la valutazione del land cover da dati MODIS nell'area mediterranea]. *Ital J Remote Sens Riv Ital di Telerilevamento* 43:19–31
- Melis MT, Afrasinei GM, Belkheir O, Carletti A, Iocola I, Pittalis D, Virdis S, Ghiglieri G (2013) Caratterizzazione spettrale delle aree interessate da salinizzazione nel bacino del Oued Biskra in Algeria a supporto delle politiche di gestione dell'acqua nell'ambito del progetto WADIS-MAR. Atti 17a Conferenza Nazionale ASITA, 5–7 November 2013, Riva del Garda Atti 17a C:977–982
- Metternicht G, Zinck JA (2008) Spectral behavior of salt types. In: Remote sensing of soil salinization. CRC Press, Boca Raton
- Mia B, Fujimitsu Y (2012) Mapping hydrothermal altered mineral deposits using Landsat 7 ETM+ image in and around Kuju volcano, Kyushu, Japan. *J Earth Syst Sci* 121:1049–1057. doi:10.1007/s12040-012-0211-9
- Mostephaoui T, Bensaid R, Saker ML (2013) Localization and delimitation of the arid soils by remote sensing and in situ measurements in an arid area: case of Oued Djedi watershed, Biskra, Algeria. *World Appl Sci J* 24:370–382. doi:10.5829/idosi.wasj.2013.24.03.972
- Msadki HD, Bouzaida DO, Taamallah H, Ouessar M (2014) Apport des données Landsat Thematic Mapper pour la cartographie des sols dans la région de Menzel Habib. *Afrique SCIENCE* 10:68–78
- Mulder VL, de Bruin S, Schaepman ME, Mayr TR (2011) The use of remote sensing in soil and terrain mapping—a review. *Geoderma* 162:1–19. doi:10.1016/j.geoderma.2010.12.018
- Muller SJ, van Niekerk A (2016a) An evaluation of supervised classifiers for indirectly detecting salt-affected areas at irrigation scheme level. *Int J Appl Earth Obs Geoinf* 49:138–150. doi:10.1016/j.jag.2016.02.005
- Muller SJ, van Niekerk A (2016b) Identification of WorldView-2 spectral and spatial factors in detecting salt accumulation in cultivated fields. *Geoderma* 273:1–11. doi:10.1016/j.geoderma.2016.02.028
- NRD WADIS-MAR (2011) WADIS-MAR Water harvesting and Agricultural techniques in Dry lands: an Integrated and Sustainable model in MAghreb Regions. WADIS-MAR Project, SWIM. <http://www.wadismar.eu/>. Accessed 20 July 2016
- NRD WADIS-MAR (2012) Projections and transformations quick guide update 03. WADIS-MAR Project, SWIM. <http://www.wadismar.eu/>. Accessed 20 July 2016
- NRD WADIS-MAR Project (2012) Metadata quick guide V1.0. WADIS-MAR Project, SWIM. <http://www.wadismar.eu/>. Accessed 9 June 2017
- Nutini F, Boschetti M, Brivio PA, Bocchi S, Antoninetti M (2013) Land-use and land-cover change detection in a semi-arid area of Niger using multi-temporal analysis of Landsat images. *Int J Remote Sens* 34:4769–4790. doi:10.1080/01431161.2013.781702
- Olofsson P, Foody GM, Herold M, Stehman SV, Woodcock CE, Wulder MA (2014) Good practices for estimating area and assessing accuracy of land change. *Remote Sens Environ* 148:42–57. doi:10.1016/j.rse.2014.02.015
- Otukey JR, Blaschke T (2010) Land cover change assessment using decision trees, support vector machines and maximum likelihood classification algorithms. *Int J Appl Earth Observ Geoinform* 12:27–31. doi:10.1016/j.jag.2009.11.002
- Ouerchefani D, Dhaou H, Delaitre E, Callot Y, Abdeljaoued S (2013) Geographic information system (GIS) and remote sensing for multi-temporal analysis of sand encroachment at Oglet Merteba (south Tunisia). *Afr J Environ Sci Technol* 7:938–943. doi:10.5897/AJEST2012.1414
- Ouessar M (2007) Hydrological impacts of rainwater harvesting in wadi Oum Zessar watershed (southern Tunisia), Ghent University
- Ouessar M, Sghaier M, Mahdhi N, Abdelli F, De Graaff J, Chaieb H, Yahyaoui H, Gabriels D (2004) An integrated approach for impact assessment of water harvesting techniques in dry areas: the case of oued Oum Zessar watershed (Tunisia). *Environ Monit Assess* 99:127–140
- Pal M (2012) Advanced algorithms for land use and cover classification. In: Advances in mapping from remote sensor imagery. CRC Press, Boca Raton, pp 69–90
- Pal M, Mather PM (2003) An assessment of the effectiveness of decision tree methods for land cover classification. *Remote Sens Environ* 86:554–565. doi:10.1016/S0034-4257(03)00132-9
- Pandey PC, Rani M, Srivastava PK, Sharma LK, Nathawat MS (2013) Land degradation severity assessment with sand encroachment in an ecologically fragile arid environment: a geospatial perspective. *QScience Connect* 43:17. doi:10.5339/connect.2013.43

- Rao P, Chen S, Sun K (2006) Improved classification of soil salinity by decision tree on remotely sensed images, p 60273 K–60273 K–8
- Rogan J, Chen D, Treitz P, Rogan J (2004) Remote sensing for mapping and monitoring land-cover and land-use change. *Progr Plann* 61:267. doi:10.1016/S0305-9006(03)00064-3
- Sadiq A, Howari F (2009) Remote sensing and spectral characteristics of desert sand from Qatar Peninsula, Arabian/Persian Gulf. *Remote Sens* 1:915–933. doi:10.3390/rs1040915
- Sarti F, ESA Earth Observation (2012) The ESA Earth Observation Programmes: status and outlook. In: ESA Radar Remote Sensing Course, Tartu, Estonia. https://earth.esa.int/c/document_library/get_file?folderId=226458&name=DLFE-2122.pdf. Accessed 9 June 2017
- Schiettecatte W, Ouassar M, Gabriels D, Tanghe S, Heirman S, Abdelli F (2005) Impact of water harvesting techniques on soil and water conservation: a case study on a micro catchment in southeastern Tunisia. *J Arid Environ* 61:297–313. doi:10.1016/j.jaridenv.2004.09.022
- Scudiero E, Skaggs TH, Corwin DL (2015) Regional-scale soil salinity assessment using Landsat ETM+ canopy reflectance. *Remote Sens Environ* 169:335–343. doi:10.1016/j.rse.2015.08.026
- Sghaier M, Ouassar M, Belgacem AO, Taamallah H (2010) Vulnerability of olive production sector to climate change in the governorate of Médenine (Tunisia). Final report. CI:GRASP project
- Sheng J, Ma L, Jiang P, Li B, Huang F, Wu H (2010) Digital soil mapping to enable classification of the salt-affected soils in desert agro-ecological zones. *Agric Water Manag* 97:1944–1951. doi:10.1016/j.agwat.2009.04.011
- Sidike A, Zhao S, Wen Y (2014) Estimating soil salinity in Pingluo County of China using QuickBird data and soil reflectance spectra. *Int J Appl Earth Obs Geoinf* 26:156–175. doi:10.1016/j.jag.2013.06.002
- Singh A (2015) Soil salinization and waterlogging: a threat to environment and agricultural sustainability. *Ecol Ind* 57:128–130. doi:10.1016/j.ecolind.2015.04.027
- Srimani PK, Prasad N (2012) Decision tree classification model for land use and land cover mapping—a case study. *Int J Curr Res* 4:177–181
- Trabelsi R, Abid K, Zouari K, Yahyaoui H (2012) Groundwater salinization processes in shallow coastal aquifer of Djefara plain of Medenine, Southeastern Tunisia. *Environ Earth Sci* 66:641–653. doi:10.1007/s12665-011-1273-8
- Triki Fourati H, Bouaziz M, Benzina M, Bouaziz S (2015) Modeling of soil salinity within a semi-arid region using spectral analysis using spectral analysis. *Arab J Geosci*. doi:10.1007/s12517-015-2004-3
- Triki H, Nationale E, Bouaziz M, Universit T (2016) Modeling of soil salinity within a semi-arid region using spectral analysis using spectral analysis. doi: 10.1007/s12517-015-2004-3
- Tutiempo Network SL World weather (historical). <http://en.tutiempo.net/>. Accessed 20 July 2016
- Vacca A, Loddo S, Melis MT, Funedda A, Puddu R, Verona M, Fanni S, Fantola F, Madrau S, Marrone VA, Serra G, Tore C, Manca D, Pasci S, Puddu MR, Schirru P (2014) A GIS based method for soil mapping in Sardinia, Italy: a geomatic approach. *J Environ Manage* 138:87–96. doi:10.1016/j.jenvman.2013.11.018
- Vanonckelen S, Lhermitte S, Balthazar V, Van Rompaey A (2014) Performance of atmospheric and topographic correction methods on Landsat imagery in mountain areas. *Int J Remote Sens* 35:4952–4972. doi:10.1080/01431161.2014.933280
- Vogiatzakis IN, Melis MT (2015) Changing perceptions in Mediterranean Geography: the role of geospatial tools. In: Theano S, Terkenli AD and LFC (eds) Connections, mobilities, urban prospects and environmental threats. The Mediterranean in Transition. Cambridge Scholars Publishing, Lady Stephenson Library, Newcastle upon Tyne, NE6 2PA, UK
- Wang H, Ma M, Geng L (2015) Monitoring the recent trend of aeolian desertification using Landsat TM and Landsat 8 imagery on the north-east Qinghai-Tibet Plateau in the Qinghai Lake basin. *Nat Hazards* 79:1753–1772. doi:10.1007/s11069-015-1924-2
- Yahiaoui I, Douaoui A, Zhang Q, Ziane A (2015) Soil salinity prediction in the Lower Cheliff plain (Algeria) based on remote sensing and topographic feature analysis. *J Arid Land* 7:794–805. doi:10.1007/s40333-015-0053-9
- Yu R, Liu T, Xu Y, Zhu C, Zhang Q, Qu Z, Liu X, Li C (2010) Analysis of salinization dynamics by remote sensing in Hetao Irrigation District of North China. *Agric Water Manag* 97:1952–1960. doi:10.1016/j.agwat.2010.03.009
- Zewdie W (2015) Remote sensing based multi-temporal land cover classification and change detection in northwestern Ethiopia. *Eur J Remote Sens*. doi:10.5721/EuJRS20154808
- Zhang Z, Wang X, Zhao X, Liu B, Yi L, Zuo L, Wen Q, Liu F, Xu J, Hu S (2014) A 2010 update of National Land Use/Cover Database of China at 1:100000 scale using medium spatial resolution satellite images. *Remote Sens Environ* 149:142–154. doi:10.1016/j.rse.2014.04.004
- Zhu Z, Woodcock CE (2014) Continuous change detection and classification of land cover using all available Landsat data. *Remote Sens Environ* 144:152–171. doi:10.1016/j.rse.2014.01.011